Cartilage
1(1) 10–19

DOI: 10.1177/1947603509354991
http://cart.sagepub.com
SAGE

Topographic Patterns of Cartilage Lesions in Knee Osteoarthritis

Won C. Bae[1], Melanie M. Payanal[2], Albert C. Chen[1], Nancy D. Hsieh-Bonassera[1], Brooke L. Ballard[1], Martin K. Lotz[3], Richard D. Coutts[1], William D. Bugbee[1,4], and Robert L. Sah[1]

Abstract

Objective: Treatments for articular cartilage lesions could benefit from characterization of lesion patterns and their progression to end-stage osteoarthritis. The objective of this study was to identify, quantitatively, topographic patterns of cartilage lesions in the human knee. *Design:* Photographs were taken of 127 unilateral distal femora (from 109 cadavers and 18 arthroplasty remnants) with full-thickness cartilage lesions. Using digital image analysis, the lesions were localized, and normalized lesion size was determined for the patellofemoral groove (PFG) and the lateral and medial femoral condyles (LFC and MFC, respectively). Samples were classified into patterns using cluster analysis of the lesion size at each compartment. For each pattern, maps showing the extent and frequency of lesions were created. *Results:* Four main patterns (a-d) were identified (each $P < 0.001$), with the lesion size varying from small (a) to large in distinct regions (b-d). Pattern b had a predominant lesion (23% area) in the MFC and smaller (<3%) lesions elsewhere. Pattern c had predominant lesions in the LFC (19%) and MFC (10%). Pattern d had a predominant lesion in the PFG (15%) and smaller lesions in the MFC (6%) and LFC (2%). The subpatterns of a (a1-a3) had relatively small lesions, with similarity between a2 and b and between a3 and d. *Conclusion:* The present methods facilitated quantitative identification of distinct topographic patterns of full-thickness cartilage lesions, based on lesion size and location. These results have implications for stratifying osteoarthritis patients using precise quantitative methods and, with additional longitudinal data, targeting cartilage treatments.

Keywords

cartilage, classification, osteoarthritis, imaging

The articular cartilage of synovial joints deteriorates with injury and disease such as osteoarthritis (OA), resulting in the formation and progression of cartilage lesions. With limited intrinsic capacity of articular cartilage to regenerate, untreated lesions, often small and focal initially, typically enlarge with time[1] and result in full-thickness lesions with increasing exposure of the subchondral bone.[2] Such lesions may exhibit topographic variations due to distinct etiologies and progression pathways. For example, varus or valgus malalignment results in degeneration of the medial or lateral tibiofemoral compartment of the knee, respectively.[3,4] Although simple patterns of cartilage lesions are well known clinically, there is a lack of a quantitative method to both classify such patterns and precisely characterize lesion size and location.

Quantitative information on lesion location and size, and predilection for progression, is useful clinically for surgical treatment of damaged articular surfaces. For example, lesion size is considered in procedures such as microfracture, which may be used for focal cartilage defects ~<2 cm^2 to stimulate reparative mesenchymal stem cells from subchondral bone.[5,6] Osteochondral autograft transplantation or autologous chondrocyte implantation is used for 2- to 8-cm^2 defects, and osteochondral allografts are used for large (>4 cm^2) or multiple lesions.[7-9] Lesion location is also considered as it may influence clinical and functional outcome.[8] For treatment of severe and large lesions in which joint resurfacing or replacement is considered, knowing the foci

[1]University of California–San Diego, La Jolla, CA, USA
[2]School of Medicine, University of Hawai'i, Honolulu, HI, USA
[3]Scripps Research Institute, La Jolla, CA, USA
[4]Scripps Clinic, La Jolla, CA, USA

Corresponding Author:
Robert L. Sah, MD, ScD, Department of Bioengineering, 9500 Gilman Drive, Mail Code 0412, University of California–San Diego, La Jolla, CA 92093-0412, USA
Email: rsah@ucsd.edu

of cartilage lesions and understanding progression pathways of lesions are important for surgical planning and evolving patient-specific treatments. For example, for procedures such as partial knee replacement[10] and modular resurfacing,[11] an important clinical issue is identification of patients with the propensity for progression in the unoperated compartment. Also, for cartilage repair procedures such as fresh allografting,[7] treatment of the predominant lesion may be augmented by knowledge of how the untreated lesion will likely grow in size and direction.

The topography of cartilage lesions and their progression pathways remains to be established for the human knee. In plain radiographs,[4,12-15] joint space narrowing in major compartments of the knee (i.e., lateral and medial tibiofemoral, patellofemoral) indicates cartilage lesions of a large size but not their precise location. Magnetic resonance imaging methods have focused primarily on cartilage volume[16,17] and described the location of the lesions typically within coarse grids.[18-20] More detailed assessment of lesion morphology has been performed with image processing for a limited number of samples.[21,22] Arthroscopy[1] and gross photography[23,24] are more sensitive[25] to small lesions than are radiographic or MRI methods, and they have been used in animal models of OA[24] to determine the location and severity of cartilage degeneration after anterior cruciate ligament injury. Direct visualization could also be used to analyze areas of full-thickness lesions of human distal femur.

Classification of individual knees based on their topography of cartilage lesions may reveal characteristic disease patterns. Cluster analysis has been used to segment a data set into groups based on the similarity of measures or features. For example, finger arthritis has been classified based on the finger(s) affected, gender, and biomarkers.[26] Analogously, knee OA could be classified based on the size of the cartilage lesions in the compartments of the joint. Once samples are classified into groups, mean lesion topographies can be determined for each group to identify characteristic patterns. Furthermore, the relationship between patterns can be assessed to infer possible progression pathways.

Certain risk factors for knee OA may be related to topographic patterns of cartilage lesions. Such risk factors include systemic factors and local mechanical factors. Systemic risk factors include age and sex, with the prevalence and incidence of knee OA increasing with age,[27-29] especially in women after the age of 50 years.[30] Mechanical risk factors include overloading, knee alignment, and joint shape. In cadaveric (CAD) specimens, joint geometry has been determined, and a shallow patellofemoral groove (PFG)[31] has been correlated with patellofemoral OA. Thus, age, sex, and patellofemoral geometry, individually and in combination, would be useful to analyze in relationship to specific patterns of knee OA.

We hypothesize that distinct topographic patterns of full-thickness cartilage lesions in the human distal femora can be identified from statistical analysis of lesion characteristics. To address this hypothesis, the objective of this study was to determine, using image processing and cluster analysis, the size, location, and extent of full-thickness cartilage lesions in the knees from cadavers and patients and to stage them to identify possible pathways of lesion advancement and disease progression. Determining the patterns and progression of cartilage lesions may help identify subtypes of knee OA based on lesion topography. Ultimately, relating lesion patterns to OA risk factors provides a basis for patient-specific treatment regimens.

Materials and Methods

Samples

Unilateral distal femora were obtained intact from 109 CAD knees and as osteochondral fragments from 18 knees after total knee arthroplasty (TKA) with institutional review board approval. A total of 70 female and 57 male specimens were available (**Table 1**). The samples were chosen based on gross observation of 1 or more full-thickness lesions of articular cartilage. Knees afflicted with rheumatoid arthritis were excluded from this study.

Photography

The CAD femora were isolated and placed in a standard position, resting on ~8 inches of femoral shaft and the posterior aspects of femoral condyles. A camera was positioned parallel (±1°) to the support surface and perpendicular to both condyles, yielding a view of the PFG and condyles (**Fig. 1A**). The major TKA fragments were positioned anatomically and photographed (**Fig. 1C**).

Lesion Localization

Photographs were digitized and opened in Photoshop (Adobe Systems Inc., San Jose, CA), and the areas representing the visible articular surface of the joint (**Figs. 1 A and C**, solid outline) and those encompassing full-thickness cartilage lesions with exposed bone (**Figs. 1 A and C**, dashed outline) were outlined. Images and outlines of the left knees were flipped horizontally to match the aspects of the right knees.

Image Processing

Image normalization. For CAD knee images (**Fig. 1A**), the outlines of joints and lesions were normalized using image processing (MATLAB 7.0 with Image Processing Toolbox, Mathworks, Natick, MA) to provide consistent and objective quantification of morphology. The joint outlines were segmented, filled, and analyzed to determine pixel

Table 1. Sample Information[a]

Pattern	Age, y (mean ± SD)	*n* (% of all patterns)				
		All specimens	Female	Male	Cadaveric knees	Total knee arthroplasty
a	68.9 ± 13.3	68 (54)	40 (57)	28 (49)	63 (58)	5 (28)
a1	65.9 ± 14.4	29 (23)	17 (24)	12 (21)	27 (25)	2 (11)
a2	72.5 ± 10.2	28 (22)	16 (23)	12 (21)	25 (23)	3 (17)
a3	67.5 ± 16.1	11 (9)	7 (10)	4 (7)	11 (10)	0 (0)
b	70.8 ± 11.6	35 (28)	15 (21)	20 (35)	25 (23)	10 (56)
c	76.7 ± 9.6	12 (9)	6 (9)	6 (11)	9 (8)	3 (17)
d	74.6 ± 11.8	12 (9)	9 (13)	3 (5)	12 (11)	0 (0)
All patterns	72.7 ± 11.6	127 (100)	70 (100)	57 (100)	109 (100)	18 (100)

[a]The tissue source was all specimens unless otherwise indicated.

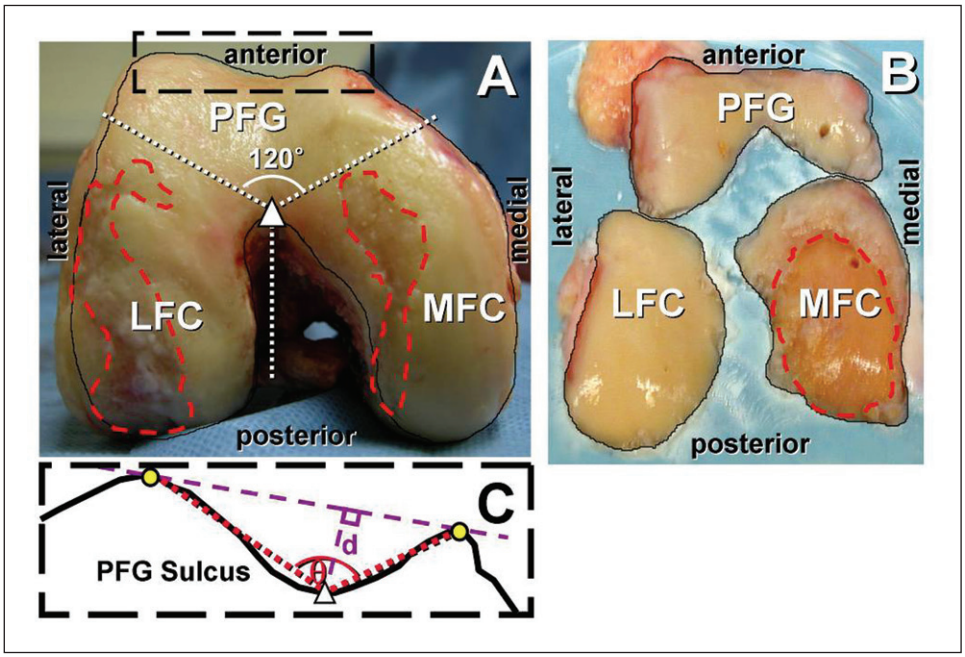

Figure 1. Localization of articular surface and full-thickness lesions and division of anatomical locations. Patellofemoral groove (PFG), lateral femoral condyle (LFC), and medial femoral condyle (MFC) in images of (**A**) cadaveric and (**B**) total knee arthroplasty samples. (**C**) Methods for measuring sulcus angle (q) and depth (d) of the patellofemoral groove of cadaveric samples.

area as well as the location of the joint centroid and the posterior peaks of the condyles. To normalize, the outlines of the joints and lesions were rotated to align the condylar peaks horizontally, translated to center the image about the centroid (the center of the image area), and scaled to the same total area (250,000 pixels, corresponding to ~2,500 mm^2 or ~0.01 mm^2/pixel area for a typical female knee[32,33]). This resulted in CAD joint outlines with the overall (i.e., widest dimension) width and height of 662 ± 23 pixels (~66 mm or ~0.1 mm/pixel length for a typical female knee[32,33]) and 543 ± 23 pixels (~54 mm), respectively.

Maps of lesions. Color maps (**Fig. 2**) showing lesion location and frequency were also computed for CAD samples in each pattern (a, b, c, d, a1, a2, and a3). The joint boundary for each pattern was determined by averaging the segmented images of the joint outline, applying a 50% threshold, filtering with a median filter (~3 × 3 mm^2). The lesion maps were created by averaging segmented images of the lesions, applying an average filter (~1 × 1 mm^2), and overlaying the joint boundary.

Size of lesions. The combined size of the lesions in each compartment, lateral femoral condyle (LFC), PFG, and the medial femoral condyle (MFC), was quantified (**Figs. 3 B and C**) in all (CAD and TKA) samples. On CAD knee images (**Fig. 3A**), the coordinate of the anterior peak of the intercondylar notch (**Fig. 1A**, triangle) was determined from the local maximum of the joint outline and used as the center point for trisecting the image into 3 regions approximating anatomical regions (**Fig. 1A**) of the LFC, PFG, and MFC. The relative size of the lesions in each region was quantified as a percentage of the total joint area. To achieve this, total number of pixels representing lesion area was divided by that representing the joint area. For TKA fragment images (**Fig. 1B**), 3 fragments covering the areas analogous to those in the CAD knee images (**Fig. 1A**) were used.

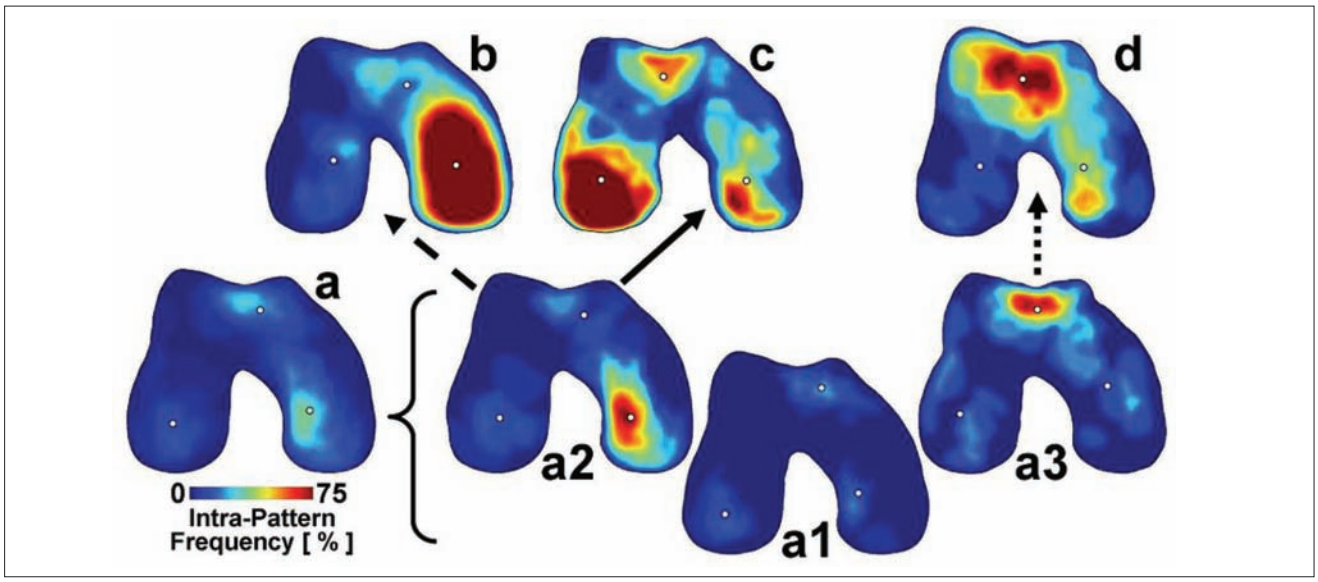

Figure 2. Maps of full-thickness lesion location and incidence for each main pattern: **a**, mixed; **b**, medial femoral condyle (MFC); **c**, lateral femoral condyle (LFC); **d**, patellofemoral groove (PFG); subpattern a1, mixed small; subpattern a2, MFC small; subpattern a3, PFG small in cadaveric samples. Dots indicate the centroid of the lesions within each anatomical location (LFC, PFG, MFC) for each pattern. Arrows indicate possible pathways of lesion progression from subpatterns to main patterns. *n* = 9 to 63.

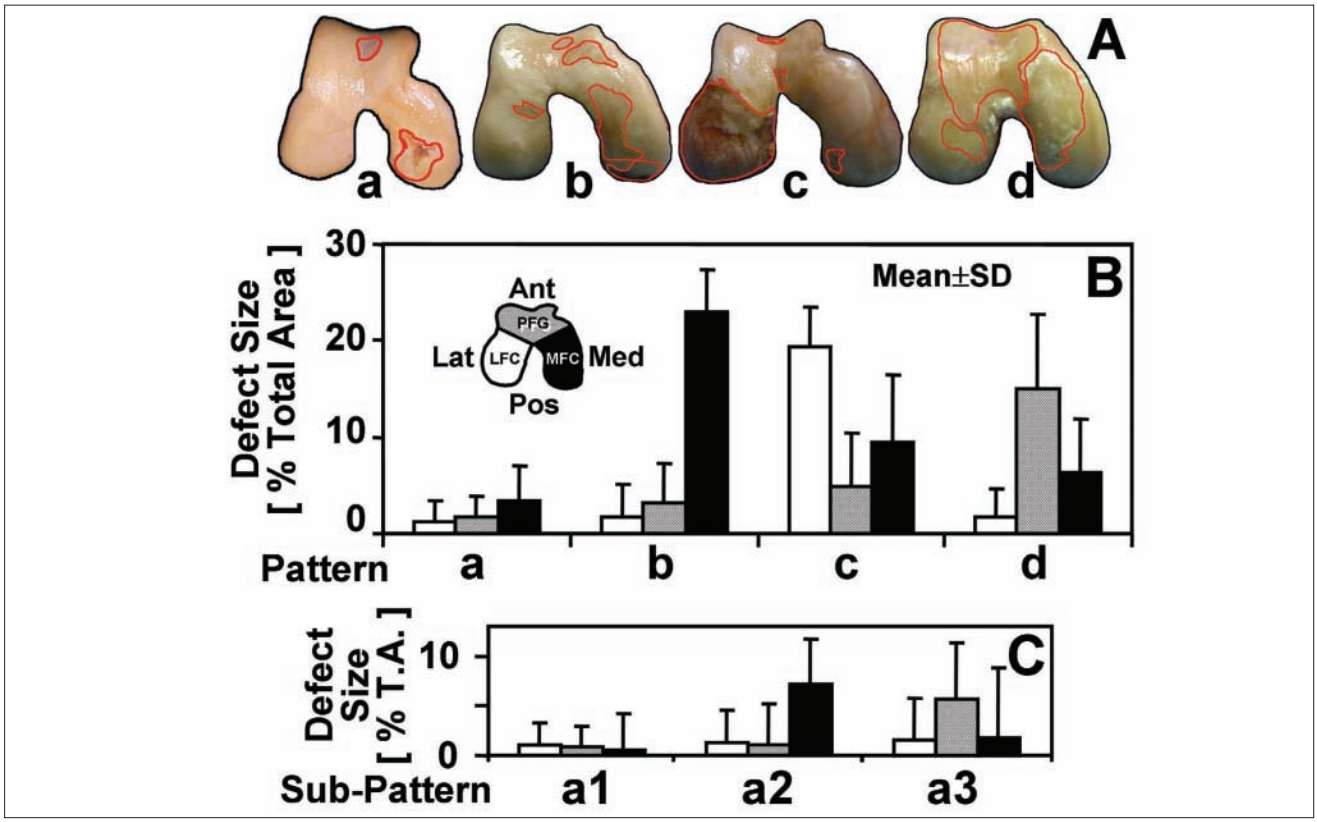

Figure 3. (**A**) representative photographs of the samples within 4 main patterns: a, mixed; b, medial femoral condyle; c, lateral femoral condyle; d, patellofemoral groove. Location-dependent size of full-thickness lesions of samples classified within (**B**) 4 main patterns and (**C**) subpatterns of a: a1, mixed small; a2, medial femoral condyle small; a3, patellofemoral groove small. *n* = 12 to 68 (see **Table 1**).

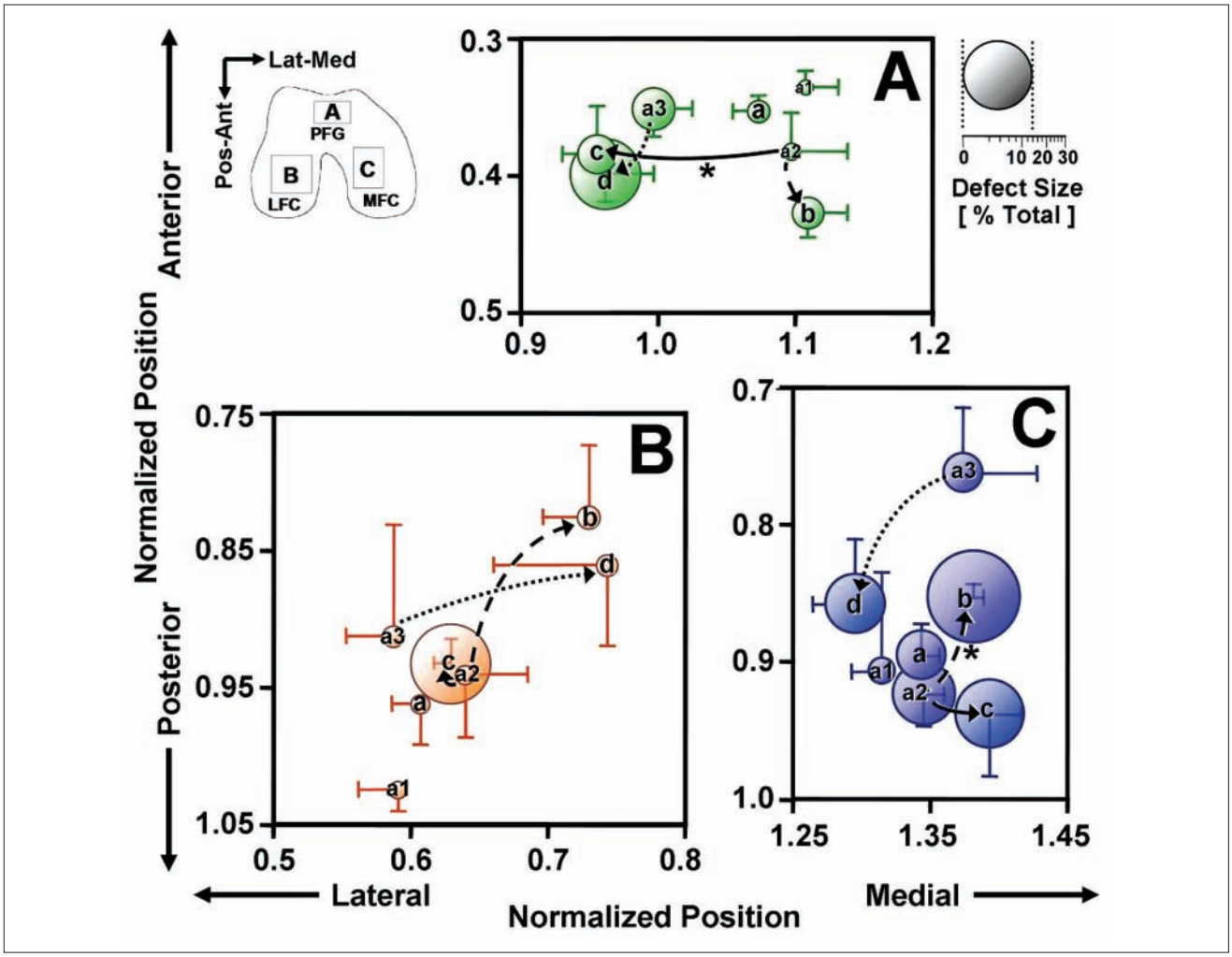

Figure 4. Centroid and size of lesions for each main pattern: a, mixed; b, medial femoral condyle (MFC); c, lateral femoral condyle (LFC); d, patellofemoral groove (PFG); subpattern a1, mixed small; subpattern a2, MFC small; subpattern a3, PFG small within each anatomical location of (**A**) PFG, (**B**) LFC, and (**C**) MFC. Arrows indicate possible pathways of lesion progression from subpatterns to main patterns. *$P < 0.05$ for differences in lesion centroid location. Mean ± SEM, $n = 5$ to 39.

Location of lesions. To quantify the location of lesions, the coordinate of centroid of the outlined areas of the lesions in each compartment, if present, was determined. To determine normalized location for the knee size, the pixel coordinates were divided by square root of the joint area (i.e., 500 pixels or ~50 mm) and plotted (**Fig. 4**). The location of lesions did not appear to be markedly influenced by joint geometry because the centroid of each joint compartment (i.e., LFC, PFG, MFC) was similar across all patterns (data not shown).

Geometry of PFG. To determine if joint geometry is associated with patterns of lesions, the shape of the PFG was assessed for the CAD samples. The locations of the anterior peaks (**Fig. 1B**, circle) and the posterior valley (**Fig. 1B**, triangle) of the PFG were determined from the local maxima and minimum, respectively, of the joint outline. From these points, the PFG's sulcus angle (**Fig. 1B**, θ) and depth (**Fig. 1B**, d) were determined, according to the definitions defined previously.[23,31] The sulcus depth was also normalized by the square root of the joint area.

Statistics

Cluster analysis. To identify major patterns of cartilage erosion in the 3 anatomical regions of the distal femur, the data of lesion size in each region were grouped using k-means cluster analysis.[34] The number of classifications (i.e., clusters) was determined using a learning algorithm[35] to determine grouping of data points assuming a Gaussian model and a statistical significance level ($\alpha < 0.01$ after Bonferroni adjustment). After cluster analysis, the percentage variance explained by the clusters and the number of samples in each cluster were determined. In addition, the

largest cluster was analyzed further by division into subclusters, using similar considerations.

Analysis of variance (ANOVA). Results are presented as mean ± SD unless noted otherwise. To assess if lesion size varied with patterns (a-d or a1-a3), considered a fixed factor, and joint location (LFC, MFC, and PFG), considered a repeated factor, repeated-measures ANOVA was used. For the given number of samples in each pattern and differences in mean values of lesion size, the power was >0.9 for all comparisons. Where significant effects ($P < 0.05$) were found, post hoc comparisons were made with appropriate Bonferroni adjustment of significance levels. The lesion size measurements were repeatable between 2 observers (intraclass correlation coefficient of 0.91; $n = 8$, 2 from each main pattern).

To assess if donor age, PFG geometry (sulcus angle and depth), and the centroids of lesions varied with the main pattern (a-d), 1-way ANOVA with the post hoc Tukey test was used.

To assess if centroids of lesions vary between subpatterns and main patterns, *t* test was performed at each anatomical location, with Bonferroni adjustment of significance.

To assess if proportions of sexes varied with main patterns (a-d), the χ^2 test was used.

Hypothesized pathways of lesion progression. To stage the lesion patterns, possible pathways of lesion progression were hypothesized based on lesion size in each compartment and under the assumption that lesions only enlarge with progression. Thus, a pattern could progress to another pattern if and only if it had smaller mean lesion sizes in every compartment compared to those in the postprogression pattern.

Results

Patterns of Lesion Topography

Cluster analysis classified 4 main patterns (referred to as a, b, c, and d) (**Figs. 2-4**). The main patterns explained ~70% of the variance in lesion sizes, with >10 samples per pattern (**Table 1**). Samples belonging to pattern a, with the largest number of samples (68), were subjected to further cluster analysis to yield 3 subpatterns (a1, a2, a3). The subpatterns explained ~60% of the variance within pattern a and contained >10 samples per subpattern (**Table 1**).

Variations in Lesion Size with Patterns

The main patterns from cluster analysis revealed quantitatively distinct lesion sizes in the 3 anatomical regions. The ANOVA indicated that lesion size (**Fig. 3B**) varied with pattern ($P < 0.001$) and anatomical regions ($P < 0.001$), with significant interaction ($P < 0.001$). Pattern a (mixed) had relatively small lesions (area of 2%-3% in each region), and it was the most abundant pattern of CAD samples (prevalence of 58%). Pattern b (MFC) had predominant lesions in the MFC (area of 23%), larger than those in the corresponding regions in patterns a (mixed), c (LFC), and d (PFG) (each $P < 0.001$); it was the pattern most prevalent in TKA samples (prevalence of 56%) and the second most abundant in the CAD samples (prevalence of 23%). Pattern c (LFC) had predominant lesions in the LFC (area of 19%), along with smaller lesions in the MFC (area of 10%) and the PFG (area of 5%); here, the LFC lesion size was larger than that in other patterns (each $P < 0.001$). Pattern d (PFG) had a large lesion size in the PFG (area of 15%) along with smaller lesions in the MFC (area of 6%); this PFG lesion size was greater than that in all other patterns (each $P < 0.001$). The effects of the pattern on sample age ($P = 0.15$) and on the proportion of sexes ($P = 0.2$) were insignificant (**Table 1**).

For each subpattern, the predominant lesions were also found in different anatomical regions. Within pattern a (mixed small), lesion size (**Fig. 3C**) varied with subpattern ($P < 0.001$) and location ($P < 0.001$), with significant interaction ($P < 0.001$). Subpatterns a2 (MFC small) and a3 (PFG small) had moderate-size (area of 6%-7%) lesions in MFC and PFG, respectively. In contrast, subpattern a1 (mixed small) had small lesions (area of 1%) in all locations. This distribution and size of lesions were consistent with photographs of representative samples (**Fig. 3A**) as well as the average lesion maps (**Fig. 2**).

Maps of Lesion Location and Frequency

The lesion maps (**Fig. 2**) indicated the extent and the location of lesions in each pattern graphically, as well as the intrapattern frequency (**Fig. 2**, color map) of lesions. The maps also included the centroid of lesions at the MFC, PFG, and LFC (**Fig. 2**, dots). For the main patterns (a-d), the predominant lesions were generally focal, and their centroid coordinates (**Fig. 4**) varied with pattern ($P < 0.01$ at each location). In the PFG (**Fig. 4A**), the centroid of pattern b (MFC) was located posterior to that of pattern a (mixed) and medial to that of patterns c (LFC) and d (PFG) (each $P < 0.05$). In the LFC (**Fig. 4B**), the centroid of pattern b was located medial to that of pattern a ($P < 0.05$). In the MFC (**Fig. 4C**), the centroid of pattern d tended to be located medial to the centroids of patterns b ($P < 0.05$) and c ($P = 0.06$).

Hypothesized Pathways of Lesion Progression and Shift in Lesion Location

Based on the lesion size in each compartment, and the assumption that lesions only enlarge with progression, the following scenarios of lesion progression were hypothesized: a1 (mixed small) can progress to any of b (MFC), c (LFC), or d (PFG); a2 (MFC small) can progress to b or

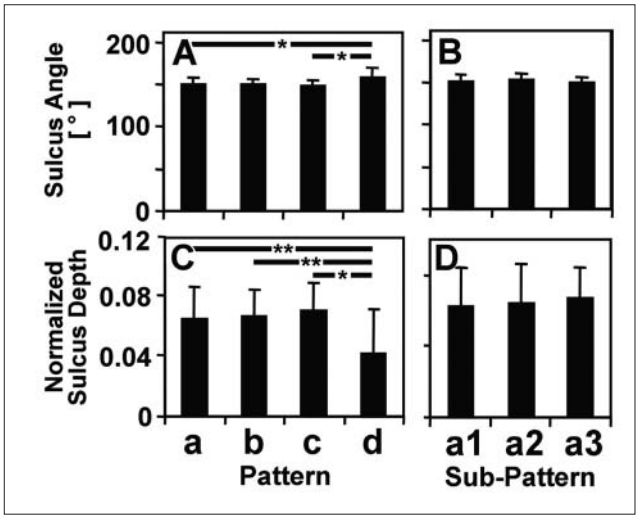

Figure 5. Sulcus (**A, B**) angle and (**C, D**) normalized depth of the patellofemoral groove in (**A, C**) main patterns and (**B, C**) subpatterns of cadaveric samples. Mean ± SD, n = 9 to 63. *$P < 0.05$. **$P < 0.01$.

c but not d; and a3 (PFG small) can progress to d but not b or c. In addition, qualitatively, pattern a2 resembled closely pattern b, whereas pattern a3 resembled pattern d.

Assuming the progression pathways from pattern a2 (MFC small) to b (MFC) or c (LFC) and from pattern a3 (PFG small) to d (PFG), the centroids of lesions in each compartment shifted with the progression. During the progression from pattern a2 to b (**Fig. 4**, dashed arrow), centroids of lesions in the PFG (**Fig. 4A**) and the MFC (**Fig. 4C**) shifted in the posterior ($P < 0.001$) and the medial ($P < 0.01$) directions, respectively. During the progression from pattern a2 to c (**Fig. 4**, solid arrow), centroids of the PFG (**Fig. 4A**) shifted laterally ($P < 0.01$), and those of the MFC (**Fig. 4C**) tended to shift medially ($P = 0.08$). From pattern a3 to d (**Fig. 4**, dotted arrow), the centroid of lesions did not shift significantly.

Variations of PFG Geometry with Patterns

Analysis of PFG sulcus angle and depth indicated that large PFG lesions but not small PFG lesions are related to PFG geometry. Both sulcus angle (**Fig. 5A**) and normalized depth (**Fig. 5C**) of the PFG varied with main pattern (each $P < 0.01$). Mean sulcus angle and normalized depth for pattern a (mixed) were 151° ± 10° and 0.064 ± 0.022, respectively (corresponding to ~6% of joint height). Pattern d (PFG) (158° ± 13° and 0.041 ± 0.021, respectively) had significantly greater angle than did patterns a (mixed) and c (LFC) (each $P < 0.05$) and shallower depth than did patterns a (mixed), b (MFC), and c (LFC) (each $P < 0.05$). For subpatterns a1 (mixed small), a2 (MFC small), and a3 (PFG small), sulcus angle (**Fig. 5B**) and normalized depth (**Fig. 5D**) were not significantly different (each $P > 0.6$).

Discussion

The present study used objective quantitative methods to identify distinct topographic patterns of full-thickness articular cartilage lesions in the human distal femora. For advanced degeneration with large full-thickness lesions, 3 distinct patterns emerged from cluster analysis: MFC degeneration (**Figs. 2 and 3**, pattern b [MFC]), posterior LFC degeneration also involving smaller lesions in the central PFG and the lateral aspect of the MFC (**Figs. 2 and 3**, pattern c [LFC]), and PFG degeneration accompanied by small lesions in the lateral aspect of the MFC (**Figs. 2 and 3**, pattern d [PFG]). Although these findings may seem obvious clinically, the present approach provides quantitative characteristics of lesion patterns. Emerging cartilage treatments such as modular resurfacing[11] require precision identification and characterization of lesions. In addition, the analysis approach may be useful for other surfaces of the knee (i.e., tibial plateau and patella), to elucidate associated patterns of degeneration.

Shortcomings of the present study include the lack of longitudinal data and clinical information, as well as inherent limitations of 2D imaging. Because harvested samples were used, the ability to directly observe the lesions was counterbalanced by an inability to analyze the time progression of lesions in individual samples. However, the sampling of >100 CAD knees (whose clinical information was unavailable), along with ~20 end-stage clinical knees, represents a reasonable spectrum of cartilage lesions at different stages of progression. It would be of interest to determine if progression pathways can be predicted from cross-sectional data. Because of the curvature of the knee, the present 2D imaging methods also could not assess the anterior- and posterior-most regions, and the lesion size from curved regions was not represented equally. Nonetheless, the imaging method provides a sensitive, straightforward, and quantitative means of assessing the topography of full-thickness lesions, one of the most prominent and frequently assessed features of OA.[18,36] Future studies using 3D imaging modalities could provide a more accurate estimate of the lesion size.

The incidence of the patterns of large lesions is consistent with and extends those of past studies. The higher incidence of the posteromedial (pattern b [MFC]) than the posterolateral (pattern c [LFC]) or patellofemoral (pattern d [PFG]) compartmental erosion is consistent with clinical observations and past studies.[12,14] Specifically, one study[12] found ~60% medial, ~15% lateral, and ~25% patellofemoral OA radiographically, similar to the proportions of patterns b, c, and d (~60%, 20%, and 20%, respectively) (**Table 1**) found in the present study. The lack of difference

in age between patterns may be owing to the selection criteria of full-thickness lesion, resulting in relatively high degeneration and age (and small range of ages) for all samples. In addition, the proportion of sexes in each pattern was not significantly different, possibly due to small number of samples in some of the patterns.

Quantification of the size and location of cartilage lesions may also aid in the deduction of progression pathways. For example, assuming that a lesion seen in pattern a2 (MFC small) progresses to b (MFC) and that in pattern a3 (PFG small) progresses to d (PFG) (**Fig. 2**), the centroids of small lesions (a2 and a3) identify sites of lesion initiation, and the centroids of larger lesions (b and d) suggest pathways of progression. Because longitudinal data were not available, to stage the identified patterns, it was assumed that lesions in each compartment only enlarged during progression. More rigorously, methods such as phylogenetic maximum likelihood analysis[37] have been used to determine evolutionary progression and pathways of humans,[38] to a known certainty. Similar methods would be useful for analysis of the shifting and enlargement of lesions, as well as initiation of new focal lesions, to establish a likely sequence of knee OA progression.

The present methods may be combined with the analysis of risk factors to determine their association with certain patterns. In the present study, an abnormal sulcus geometry in the PFG, that is, wide angle (**Fig. 5A**) and shallow depth (**Fig. 5C**) of the sulcus, was found in pattern d (PFG), consistent with past studies that associated abnormal PFG geometries and mechanical instability with degeneration in the PFG.[31] It would be useful to determine if the abnormal geometry is a predisposition to, or a consequence of, PFG degeneration. The mechanisms of lesion progression remain to be elucidated, however, and may involve a variety of mechanical factors such as high magnitude of strain,[39,40] load repetition,[39,41,42] and poor lubrication,[43] as well as biological factors such as synovial inflammation[44] and increased expression of proinflammatory cytokines.[45] Future extension of this study could also address additional risk factors, such as previous trauma, knee alignment, weight, and sex.

Ultimately, defining patterns and pathways of cartilage degeneration may be useful for stratification of patients for specific and appropriate treatments of cartilage degeneration and OA. Although many risk factors of OA have been proposed,[13,30,46-48] it remains to be determined if risk factors of OA progression are related to specific pathways. Correlation of the specific risk factors with a particular pattern of OA in future studies would allow for targeted diagnoses and treatment regimens. For example, if different physical activities are associated with unique lesion patterns, behavior modification therapies could be tailored to each patient. In addition, as customized or patient-specific surgical instruments and implants are being developed, information regarding not only the shape and size of the joint[49] but also the pattern of cartilage deficiency can be useful in the design and manufacturing of biologic and prosthetic implants. Also, understanding early patterns of lesions and their propensity for progression would help in the decision of whether to treat a small lesion. With additional data yielding more detailed and extensive maps of lesions, along with risk factors, multiple pathways of OA progression may be revealed and used to better understand and treat OA.

Declaration of Conflicting Interests

The author(s) declared no potential conflicts of interests with respect to the authorship and/or publication of this article.

Funding

This work was supported by grants from the National Institutes of Health (F32 AR054248 to WCB, P01 AG007996, R01 AR051565, T35 AG026757), the National Science Foundation, and the Howard Hughes Medical Institute through the HHMI Professors Program (to the University of California–San Diego in support of RLS).

References

1. Hjelle K, Solheim E, Strand T, Muri R, Brittberg M. Articular cartilage defects in 1,000 knee arthroscopies. Arthroscopy. 2002;18:730-4.
2. Bennett GA, Waine H, Bauer W. Changes in the knee joint at various ages with particular reference to the nature and development of degenerative joint disease. New York: Commonwealth Fund; 1942. p. 97
3. Sharma L, Song J, Felson DT, Cahue S, Shamiyeh E, Dunlop DD. The role of knee alignment in disease progression and functional decline in knee osteoarthritis. JAMA. 2001; 286:188-95.
4. Cooke D, Scudamore A, Li J, Wyss U, Bryant T, Costigan P. Axial lower-limb alignment: comparison of knee geometry in normal volunteers and osteoarthritis patients. Osteoarthritis Cartilage. 1997;5:39-47.
5. Buckwalter JA, Mankin HJ. Articular cartilage: degeneration and osteoarthritis, repair, regeneration, and transplantation. Instr Course Lect. 1998;47:487-504.
6. Steadman JR, Rodkey WG, Briggs KK. Microfracture to treat full-thickness chondral defects: surgical technique, rehabilitation, and outcomes. J Knee Surg. 2002;15:170-6.
7. Bugbee WD. Osteochondral allograft transplantation. In: Cole BJ, Malek MM, editors. Articular cartilage lesions: a practical guide to assessment and treatment. New York: Springer; 2004. p. 82-94.
8. Brittberg M. Autologous chondrocyte transplantation. Clin Orthop Relat Res. 1999;367S:147-55.
9. Hangody L, Feczko P, Bartha L, Bodo G, Kish G. Mosaicplasty for the treatment of articular defects of the knee and ankle. Clin Orthop Relat Res. 2001;391:328-336.
10. Obeid EMH, Adams MA, Newman JH. Mechanical properties of articular cartilage in knees with unicompartmental osteoarthritis. J Bone Joint Surg Br. 1994;76B:315-9.

11. Fitz W. Unicompartmental knee arthroplasty with use of novel patient-specific resurfacing implants and personalized jigs. J Bone Joint Surg Am. 2009;91(suppl 1):69-76.
12. Davies AP, Vince AS, Shepstone L, Donell ST, Glasgow MM. The radiologic prevalence of patellofemoral osteoarthritis. Clin Orthop Relat Res. 2002;402:206-12.
13. Felson DT, Zhang Y, Hannan MT, Naimark A, Weissman B, Aliabadi P, et al. Risk factors for incident radiographic knee osteoarthritis in the elderly: the Framingham study. Arthritis Rheum. 1997;40:728-33.
14. Hernborg JS, Nilsson BE. The natural course of untreated osteoarthritis of the knee. Clin Orthop Relat Res. 1977;123:130-7.
15. Englund M, Lohmander LS. Patellofemoral osteoarthritis coexistent with tibiofemoral osteoarthritis in a meniscectomy population. Ann Rheum Dis. 2005;64:1721-6.
16. Eckstein F, Reiser M, Englmeier KH, Putz R. In vivo morphometry and functional analysis of human articular cartilage with quantitative magnetic resonance imaging: from image to data, from data to theory. Anat Embryol (Berl). 2001;203: 147-73.
17. Eckstein F, Lemberger B, Gratzke C, Hudelmaier M, Glaser C, Englmeier KH, et al. In vivo cartilage deformation after different types of activity and its dependence on physical training status. Ann Rheum Dis. 2005;64:291-5.
18. Vande Berg BC, Lecouvet FE, Malghem J. Frequency and topography of lesions of the femoro-tibial cartilage at spiral CT arthrography of the knee: a study in patients with normal knee radiographs and without history of trauma. Skeletal Radiol. 2002;31:643-9.
19. Brittberg M, Winalski CS. Evaluation of cartilage injuries and repair. J Bone Joint Surg Am. 2003;85A(suppl 2):58-69.
20. Peterfy CG, Guermazi A, Zaim S, Tirman PF, Miaux Y, White D, et al. Whole-organ magnetic resonance imaging score (WORMS) of the knee in osteoarthritis. Osteoarthritis Cartilage. 2004;12:177-90.
21. Graichen H, Al-Shamari D, Hinterwimmer S, von Eisenhart-Rothe R, Vogl T, Eckstein F. Accuracy of quantitative magnetic resonance imaging in the detection of ex vivo focal cartilage defects. Ann Rheum Dis. 2005;64:1120-5.
22. Cohen ZA, Mow VC, Henry JH, Levine WN, Ateshian GA. Templates of the cartilage layers of the patellofemoral joint and their use in the assessment of osteoarthritic cartilage damage. Osteoarthritis Cartilage. 2003;11:569-79.
23. Casscells SW. Gross pathological changes in the knee joint of the aged individual: a study of 300 cases. Clin Orthop Relat Res. 1978;132:225-32.
24. Chang DG, Iverson EP, Schinagl RM, Sonoda M, Amiel D, Coutts RD, et al. Quantitation and localization of cartilage degeneration following the induction of osteoarthritis in the rabbit knee. Osteoarthritis Cartilage. 1997;5:357-72.
25. Wada M, Baba H, Imura S, Morita A, Kusaka Y. Relationship between radiographic classification and arthroscopic findings of articular cartilage lesions in osteoarthritis of the knee. Clin Exp Rheumatol. 1998;16:15-20.
26. Koo T, Nagy Z, Sesztak M, Ujfalussy I, Meretey K, Bohm U, et al. Subsets in psoriatic arthritis formed by cluster analysis. Clin Rheumatol. 2001;20:36-43.
27. Felson DT, Zhang Y, Hannan MT, Naimark A, Weissman BN, Aliabadi P, et al. The incidence and natural history of knee osteoarthritis in the elderly: the Framingham Osteoarthritis Study. Arthritis Rheum. 1995;38:1500-5.
28. Lawrence JS, Bremner JM, Bier F. Osteo-arthrosis: prevalence in the population and relationship between symptoms and x-ray changes. Ann Rheum Dis. 1966;25:1-24.
29. Felson DT, Naimark A, Anderson J, Kazis L, Castelli W, Meenan RF. The prevalence of knee osteoarthritis in the elderly: the Framingham Osteoarthritis Study. Arthritis Rheum. 1987;30:914-8.
30. Oliveria SA, Felson DT, Reed JI, Cirillo PA, Walker AM. Incidence of symptomatic hand, hip, and knee osteoarthritis among patients in a health maintenance organization. Arthritis Rheum. 1995;38:1134-41.
31. Kalichman L, Zhang Y, Niu J, Goggins J, Gale D, Felson DT, et al. The association between patellar alignment and patellofemoral joint osteoarthritis features: an MRI study. Rheumatology (Oxford). 2007;46:1303-8.
32. Hitt K, Shurman JR II, Greene K, McCarthy J, Moskal J, Hoeman T, et al. Anthropometric measurements of the human knee: correlation to the sizing of current knee arthroplasty systems. J Bone Joint Surg Am. 2003;85A (suppl 4): 115-22.
33. Conley S, Rosenberg A, Crowninshield R. The female knee: anatomic variations. J Am Acad Orthop Surg. 2007;15(suppl 1): S31-6.
34. MacQueen JB. Some methods for classification and analysis of multivariate observations. Proceedings of 5th Berkeley Symposium on Mathematical Statistics and Probability. 1967;1:281-97.
35. Hamerly G, Elkan C. Learning the k in k-means. In: Advances in neural information processing systems; Vol. 17. Cambridge, MA: MIT Press; 2003.
36. Weidow J, Pak J, Karrholm J. Different patterns of cartilage wear in medial and lateral gonarthrosis. Acta Orthop Scand. 2002;73:326-9.
37. Felsenstein J. Maximum-likelihood estimation of evolutionary trees from continuous characters. Am J Hum Genet. 1973; 25:471-92.
38. Strait DS, Grine FE. Inferring hominoid and early hominid phylogeny using craniodental characters: the role of fossil taxa. J Hum Evol. 2004;47:399-452.
39. Bae WC, Schumacher BL, Sah RL. Indentation probing of human articular cartilage: effect on chondrocyte viability. Osteoarthritis Cartilage. 2007;15:9-18.
40. Patwari P, Fay J, Cook MN, Badger AM, Kerin AJ, Lark MW, et al. In vitro models for investigation of the effects of acute mechanical injury on cartilage. Clin Orthop Relat Res. 2001; 391(suppl):S61-71.

41. Chen CT, Burton-Wurster N, Borden C, Hueffer K, Bloom SE, Lust G. Chondrocyte necrosis and apoptosis in impact damaged articular cartilage. J Orthop Res. 2001;19: 703-11.
42. Levin A, Burton-Wurster N, Chen CT, Lust G. Intercellular signaling as a cause of cell death in cyclically impacted cartilage explants. Osteoarthritis Cartilage. 2001;9:702-11.
43. Jay GD, Torres JR, Rhee DK, Helminen HJ, Hytinnen MM, Cha CJ, et al. Association between friction and wear in diarthrodial joints lacking lubricin. Arthritis Rheum. 2007;56: 3662-9.
44. Benito MJ, Veale DJ, FitzGerald O, van den Berg WB, Bresnihan B. Synovial tissue inflammation in early and late osteoarthritis. Ann Rheum Dis. 2005;64:1263-7.
45. Tetlow LC, Adlam DJ, Woolley DE. Matrix metalloproteinase and proinflammatory cytokine production by chondrocytes of human osteoarthritic cartilage: associations with degenerative changes. Arthritis Rheum. 2001;44:585-94.
46. Felson DT. Obesity and osteoarthritis of the knee. Bull Rheum Dis. 1992;41:6-7.
47. Nevitt MC, Felson DT. Sex hormones and the risk of osteoarthritis in women: epidemiological evidence. Ann Rheum Dis. 1996;55:673-6.
48. Palotie A, Vaisanen P, Ott J, Ryhanen L, Elima K, Vikkula M, et al. Predisposition to familial osteoarthrosis linked to type II collagen gene. Lancet. 1989;1:924-7.
49. Weng HH, Fitzgerald J. Current issues in joint replacement surgery. Curr Opin Rheumatol. 2006;18:163-9.